Supporting Information

How does the mono–triazole derivative modulate Aβ$_{42}$ aggregation and disrupt protofibril structure: Insights from molecular dynamics simulations

Amandeep Kaur,[a] Anupamjeet Kaur,[a] Deepti Goyal*[a] and Bhupesh Goyal*[b]

[a]*Department of Chemistry, Faculty of Basic and Applied Sciences, Sri Guru Granth Sahib World University, Fatehgarh Sahib–140406, Punjab, India*
[b]*School of Chemistry & Biochemistry, Thapar Institute of Engineering & Technology, Patiala–147004, Punjab, India*

*Corresponding authors

E–mail: bhupesh@thapar.edu; deeptig@iitbombay.org

Table of contents

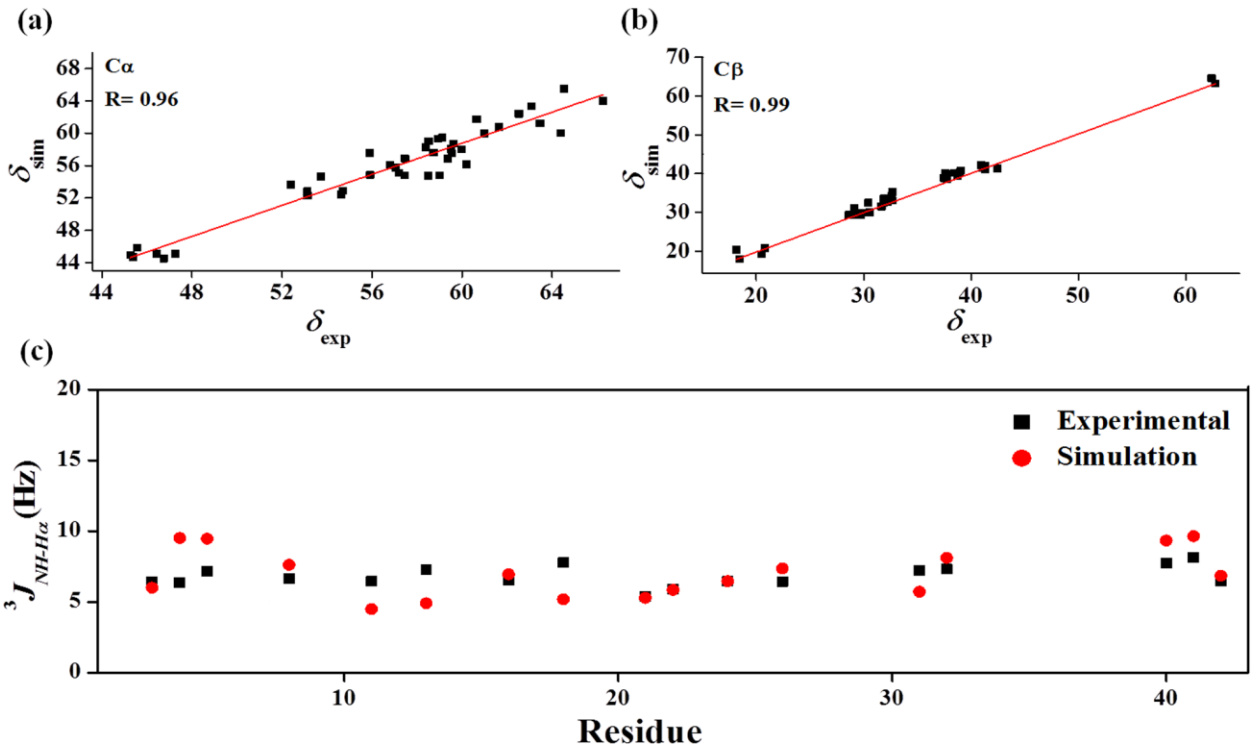

Figure S1. The correlation between simulated and experimental NMR chemical shifts for Cα and Cβ atoms of $A\beta_{42}$ monomer is shown in panel a and b, respectively. The $^{3}J_{NH-H\alpha}$ coupling constants values of $A\beta_{42}$ monomer residues obtained from the simulation and experimental data is shown in panel c.

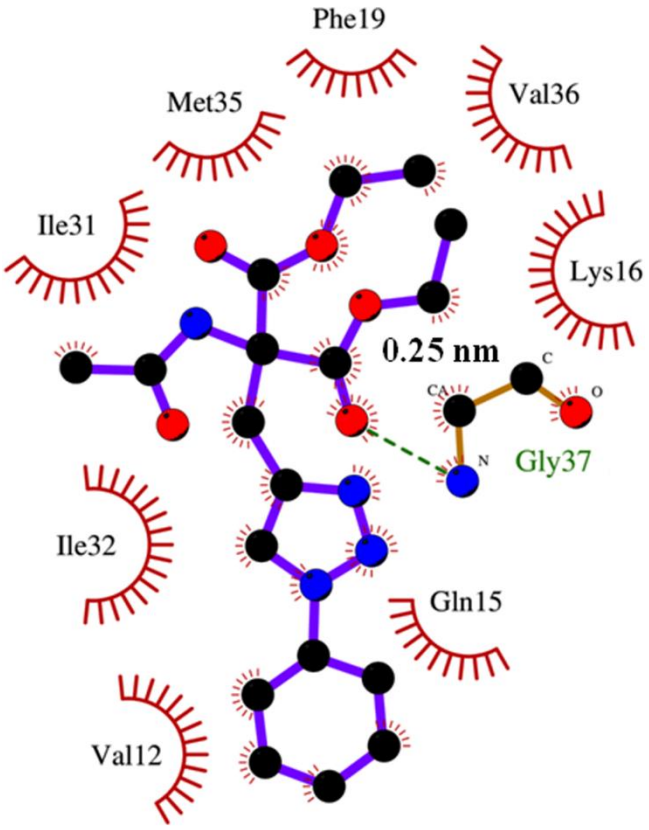

Figure S2. The 2D LigPlot^{+} map of the representative member of cluster 1 in Aβ_{42} monomer–**4v** complex displaying the hydrophobic contacts of **4v** with Aβ_{42} monomer residues. A hydrogen bond (0.25 nm) was observed between the oxygen atom of –C=O group of ester of **4v** with the backbone NH of Gly37 of Aβ_{42} monomer.

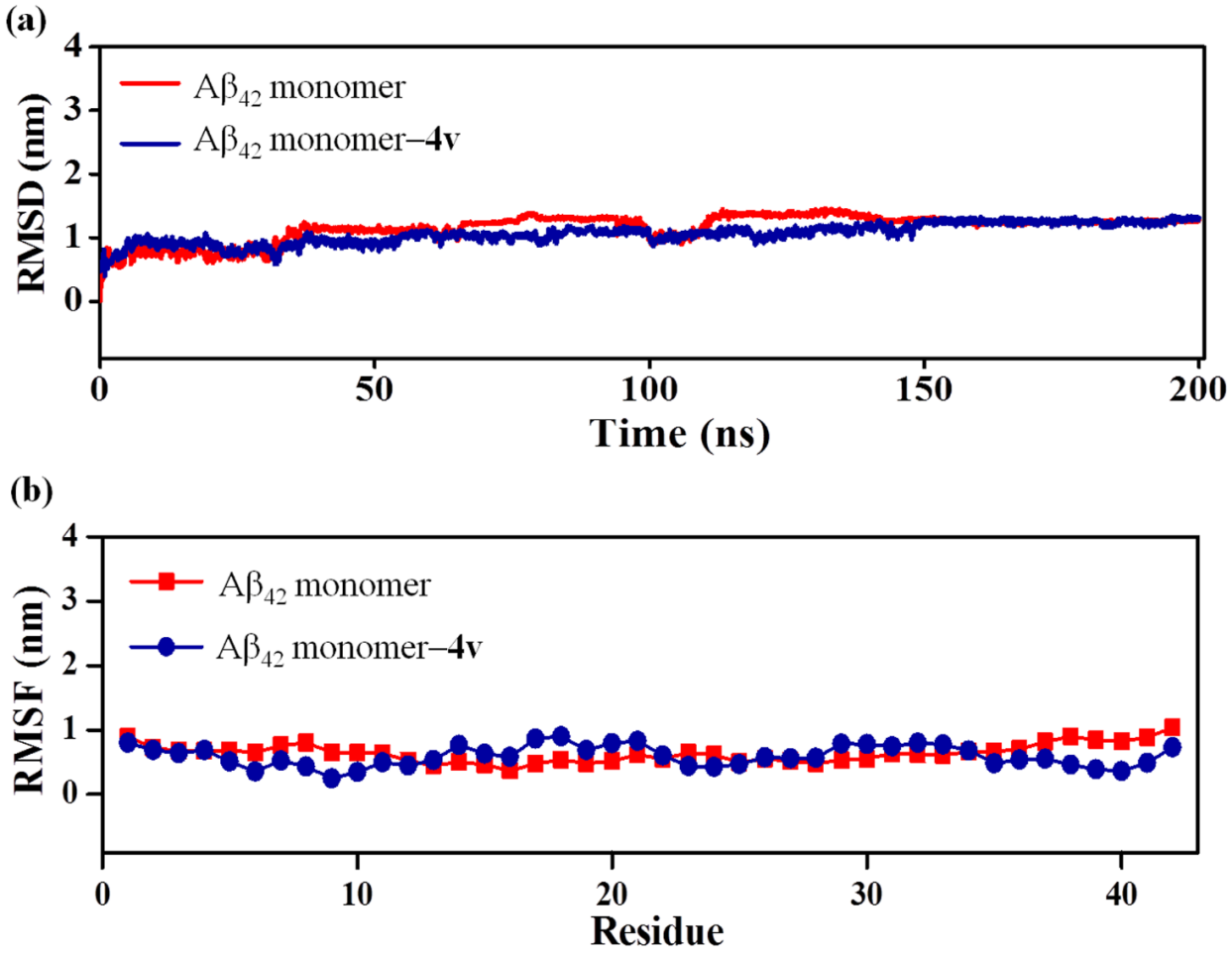

Figure S3. The root–mean–square deviation (RMSD) and root–mean–square fluctuation (RMSF) of $A\beta_{42}$ monomer (red) and $A\beta_{42}$ monomer–**4v** complex (blue) during simulation are shown in panel a and b, respectively.

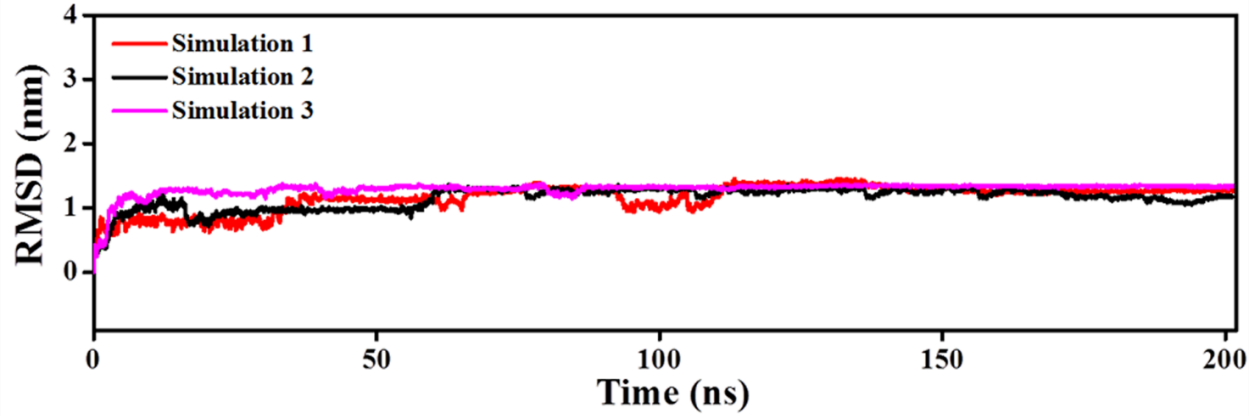

Figure S4. The RMSD of the triplicate simulations of $A\beta_{42}$ monomer is shown.

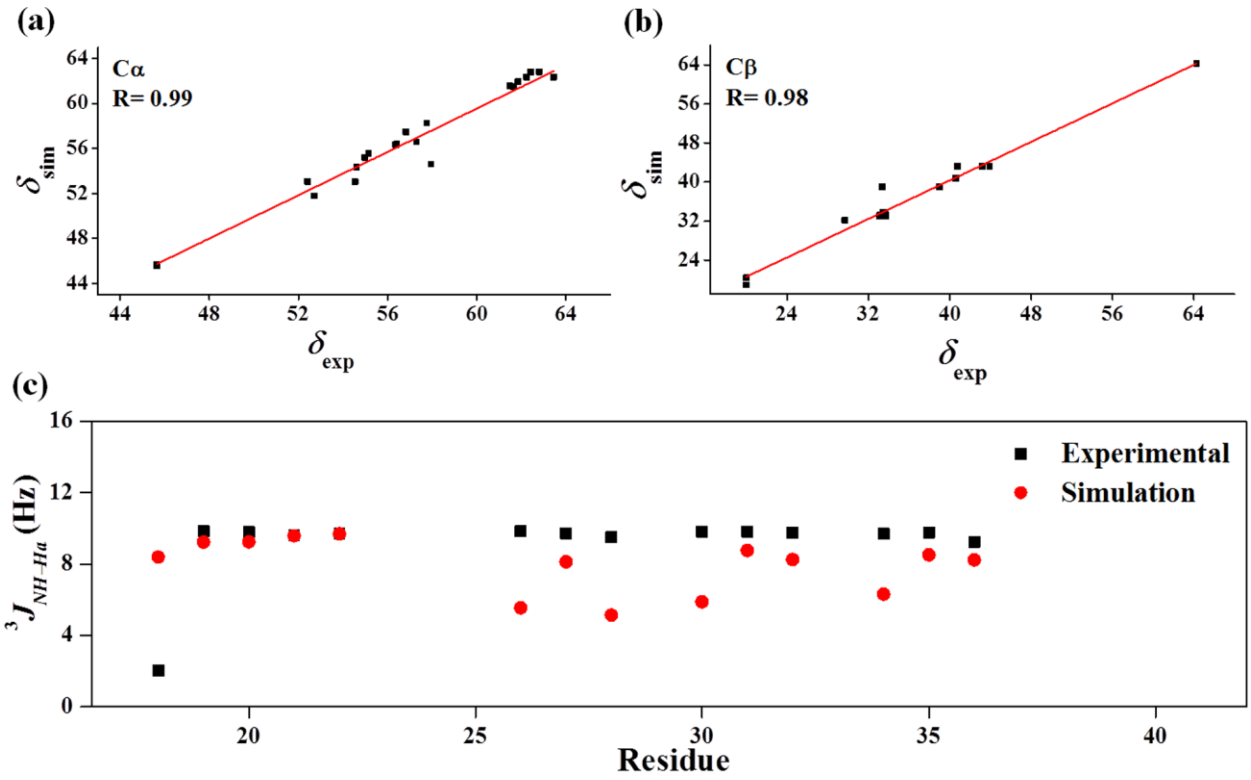

Figure S5. The correlation between simulated and experimental NMR chemical shifts for Cα and Cβ atoms of $A\beta_{42}$ protofibril is shown in panel a and b, respectively. The $^{3}J_{NH-H\alpha}$ coupling constants values of $A\beta_{42}$ protofibril residues obtained from the simulation and experimental data is shown in panel c.

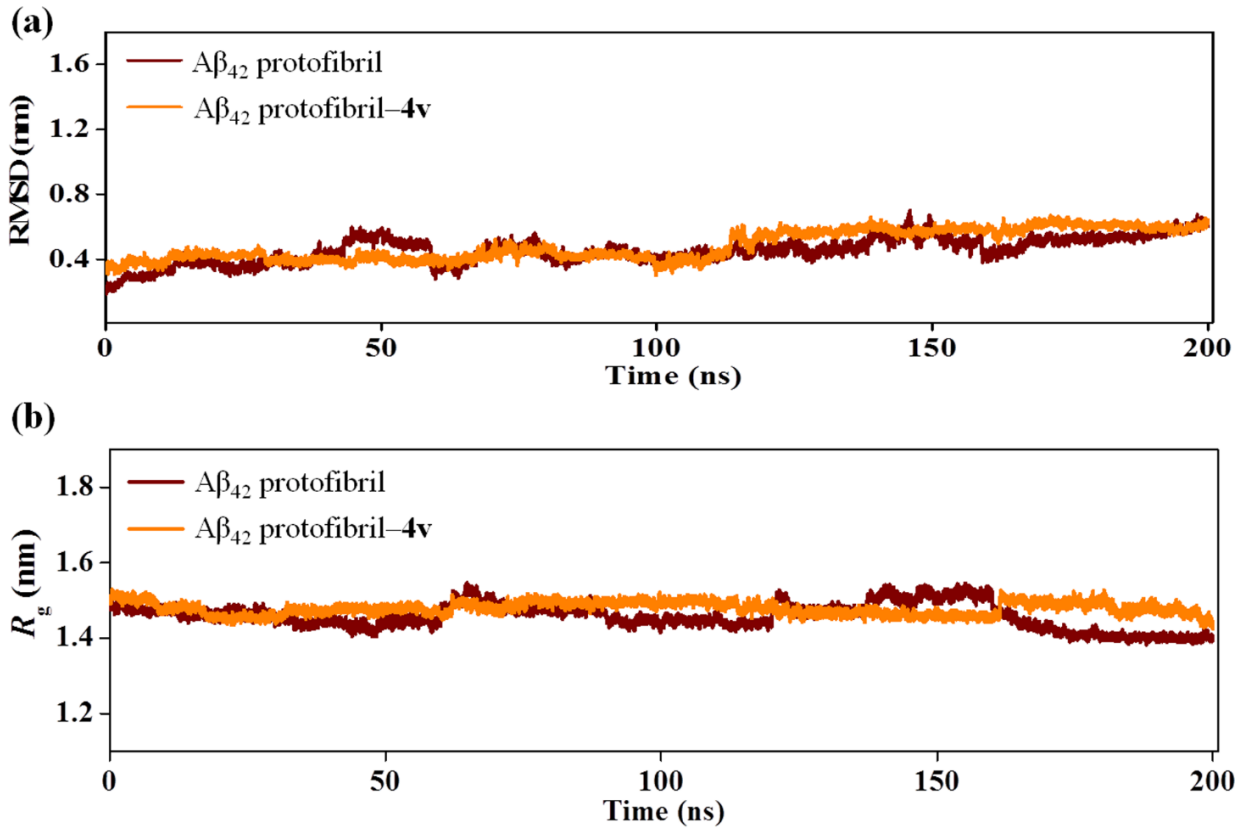

Figure S6. The RMSD and radius-of-gyration (R_g) of $A\beta_{42}$ protofibril (wine) and $A\beta_{42}$ protofibril–**4v** complex (orange) during simulation are shown in panel a and b, respectively.

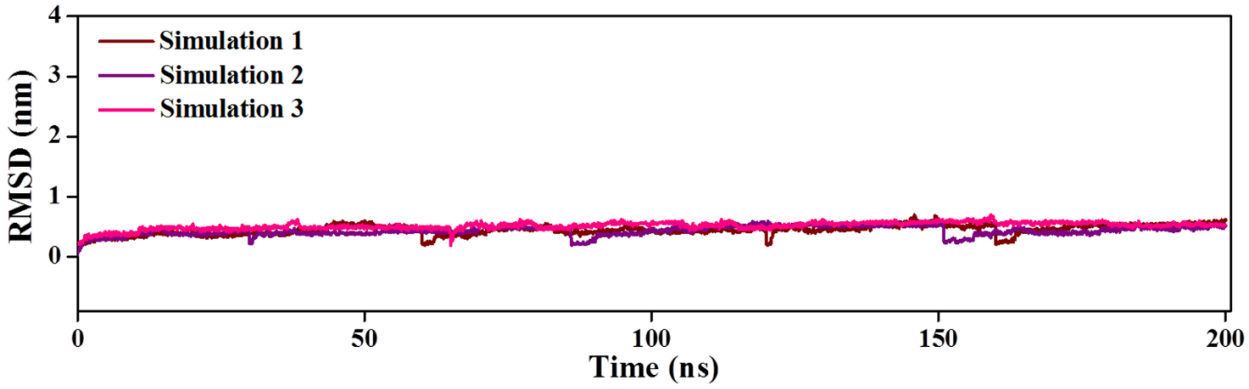

Figure S7. The RMSD of the triplicate simulations of $A\beta_{42}$ protofibril is shown.

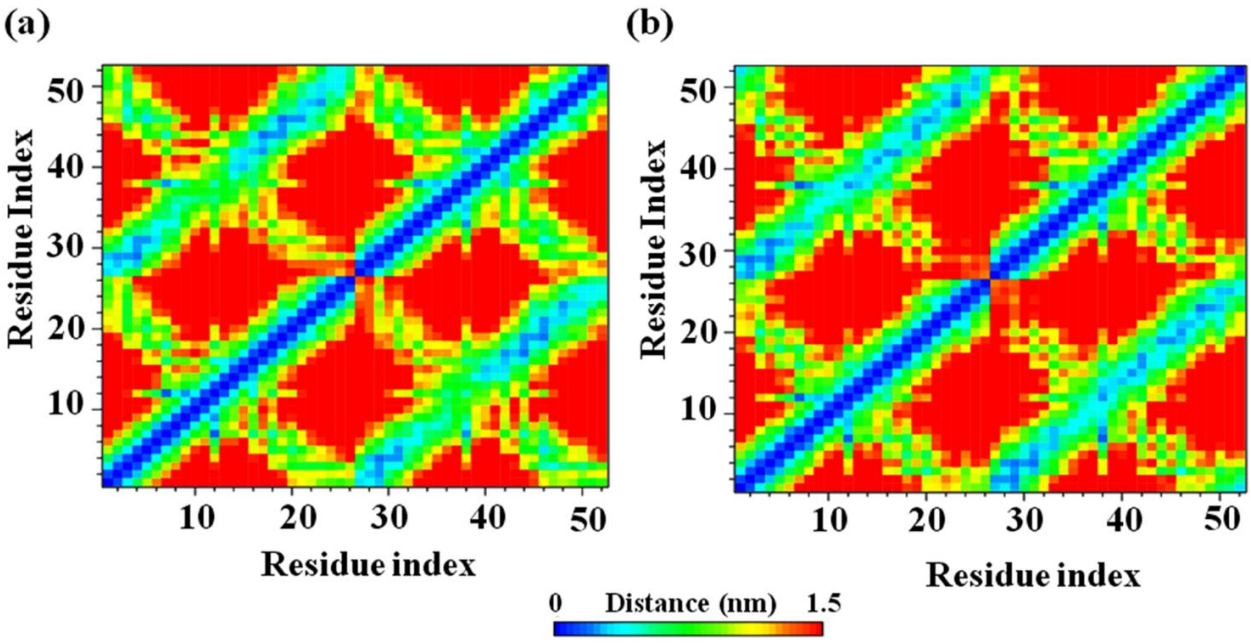

Figure S8. The residue–residue contact map of chain D and E of $A\beta_{42}$ protofibril in $A\beta_{42}$ protofibril and $A\beta_{42}$ protofibril–**4v** complex is shown in panel a and b, respectively.

Table S1. The secondary structure component statistics of $A\beta_{42}$ monomer and $A\beta_{42}$ protofibril for triplicate MD simulations. The standard errors of the mean were calculated by dividing the simulation data into four long, non-overlapping blocks.

Model system	Simulation	Secondary structure component (%)					
		Coil	[a]β–sheet	Bend	Turn	[b]Helix	Chain_ Seperator
$A\beta_{42}$ monomer	1	22.5 ± 2.8	9.0 ± 2.9	19.2 ± 3.7	24.2 ± 1.4	27.0 ± 5.1	0
	2	26.7 ± 0.6	9.7 ± 2.9	25.0 ± 3.2	15.0 ± 1.9	23.2 ± 3.5	0
	3	20.7 ± 0.7	10.5 ±1.5	17.0 ± 0.4	26.5 ± 0.6	25.0 ± 1.4	0
$A\beta_{42}$ protofibril	1	32.7 ± 1.2	54.5 ± 1.9	9.5 ± 0.6	0.2 ± 0.2	0	3.0 ± 0
	2	31.7 ± 1.7	56.2 ± 1.6	8.5 ± 0.2	0.2 ± 0.2	0	3.0 ± 0
	3	37.2 ± 3.1	48.7 ± 3.9	10.7 ± 1.3	0.5 ± 0.2	0	3.0 ± 0

[a]β–sheet= β–strand + β–bridge; [b]Helix= α–helix + 3_{10}–helix + π–helix